North Carolina State University
Department of Nuclear Engineering

MOOSE Project

On

NE – 533 Nuclear Fuel Performance

Title:

Analysis of Nuclear Fuel Using MOOSE

By

Ogechukwu Joy Ozoani

Course Instructor: Dr Benjamin Beeler

February, 2025.

1. Introduction

This report details the numerical modeling of heat conduction in a cylindrical nuclear fuel pellet using MOOSE (Multiphysics Object Oriented Simulation Environment). The problem is formulated in a 2D RZ coordinate system and solved for both steady-state and transient conditions with constant and temperature-dependent thermal conductivity. Analytical solutions are used for comparison with the steady state numerical results. The peak temperature values were shown for the transient part.

2. Problem Description

The fuel pellet geometry Fig.1. consists of:

Fuel region: Radius = 0.5 cm

Gap region: Thickness = 0.005 cm

Cladding region: Thickness = 0.1 cm

Height: 1 cm

Outer cladding temperature: 550 K

Linear Heat Rate (LHR):

- Steady state: 350 W/cm
- Transient: $350 \times \exp(-((t-20)^2) \div 2) + 350$

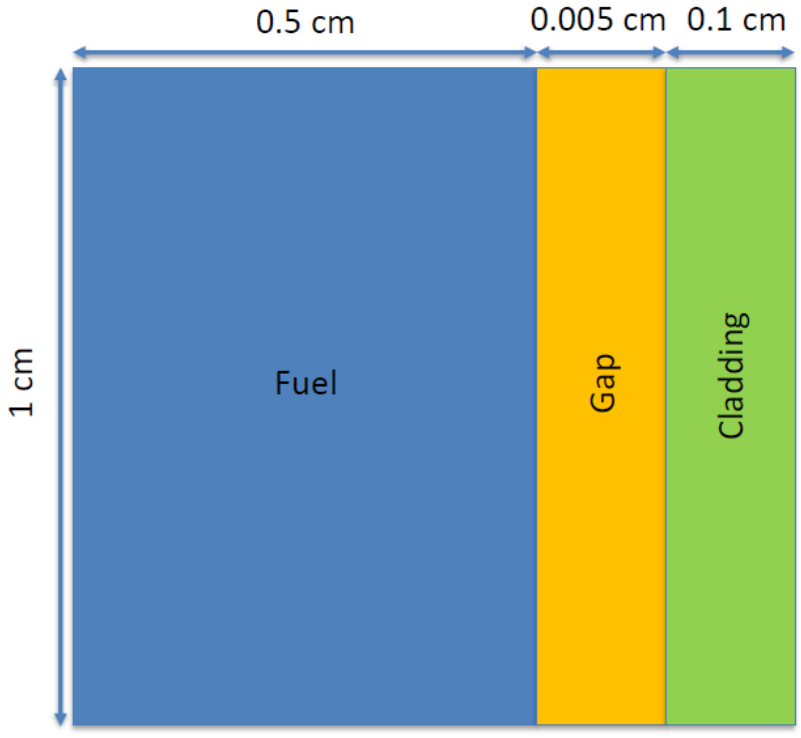

Fig.1. Problem Definition and Geometry

3. Simulation Setup

3.1. Materials selection

The materials selected for the simulation for both steady state and transient with constant thermal conductivity represent typical components of a nuclear fuel rod:

- Fuel: Thermal conductivity of 0.03 W/cm-K, typical for uranium dioxide (UO_2) at operating conditions. [1]
- Gap: Filled with helium gas, having a thermal conductivity of 0.02334 W/cm-K, For pure He: $k_{gap} = 16x10\text{^} - 6 * T\text{^}0.79$ [1]
- Cladding: Made of zirconium alloy, with a thermal conductivity of 0.17 W/cm-K, providing structural integrity and efficient heat dissipation. [1]

The materials selected for the simulation for both steady state and transient with temperature-dependent thermal conductivity were different except for the Gap:

- Fuel: Fink Model was considered given that MOOSE uses this model for UO2Thermal type [1] , [3]

The Fink equation: $k_{95} = (\frac{100}{7.5408+17.692T_n+3.6142T_n} + \left(\frac{6400}{T_n^{5/2}}\right)\exp\left(-\frac{16.35}{T_n}\right))$

Where $T_n = T/1000$

$$k = k_{95}\left(\frac{1}{1 - (2.6 - 0.5T_n)0.05}\right) = 0.0616W/cm - K$$

- Cladding: Thermal conductivity for zircaloy T range in K 298 ≤ T < 1800 [4]

$$k(T) = A0 + A1 \times \left(\frac{T}{1000}\right) + A2 \times (\frac{T}{1000})^2 = 0.1519W/cm - K$$

Where A0 = 12.767; A1 = -0.54348; A2 = 8.9818 are constants

3.2. Mesh selection

The mesh is structured as a 2D radial-axial model in rz coordinates, consisting of:

- A structured mesh with 660 radial elements and 1 axial element (QUAD4)
- Three subdomains: fuel, gap, and cladding

The resolution ensures a fine enough discretization to capture temperature gradients.

3.3. Variables

Temperature was defined. First-order elements were used for temperature interpolation. And Lagrange finite element family was used and since it uses nodal basis functions, the temperature was interpolated at the element nodes.

3.4. Kernels

ADHeatConduction type was used for both steady state and transient. It implements Fourier's law for heat conduction, ensuring temperature diffusion is modeled correctly:

$$\nabla \cdot (k\nabla T) = Q$$

The kernel consists of heat source block with type HeatSource which represents an external heat source term. This ensures localized heating in the fuel block.

ADHeatConductionTimeDerivative was considered since it represents the transient behavior of temperature, accounting for heat accumulation over time. The governing equation includes a time-dependent term:

$$\rho_{cp} = \frac{\partial t}{\partial T} = \nabla \cdot (k\nabla T) + \mathrm{q}$$

3.5. Boundary and Initial Conditions

- Initial Temperature: 550 K (applied to the entire domain).
- Neumann BC at centerline (left boundary): Zero heat flux, ensuring symmetry.
- Dirichlet BC at outer cladding (right boundary): Fixed at 550 K, representing the outer cladding temperature.

Post-processors were implemented to extract the centerline temperature. The Newton solve-type was used to execute because it utilizes the Newton-Raphson method for solving nonlinear equations. Finally, CSV type was considered to generate output in CSV format

4. Results and Discussion

The simulation was run in MOOSE, and the temperature distribution was visualized using Paraview. The graphical results were generated using MATLAB.

4.1. Steady-state with constant thermal conductivity and steady-state with temperature-dependent thermal conductivity

The steady-state temperature distribution was obtained using MOOSE under two different thermal conductivity assumptions: constant and temperature-dependent thermal conductivity.

Visualization:

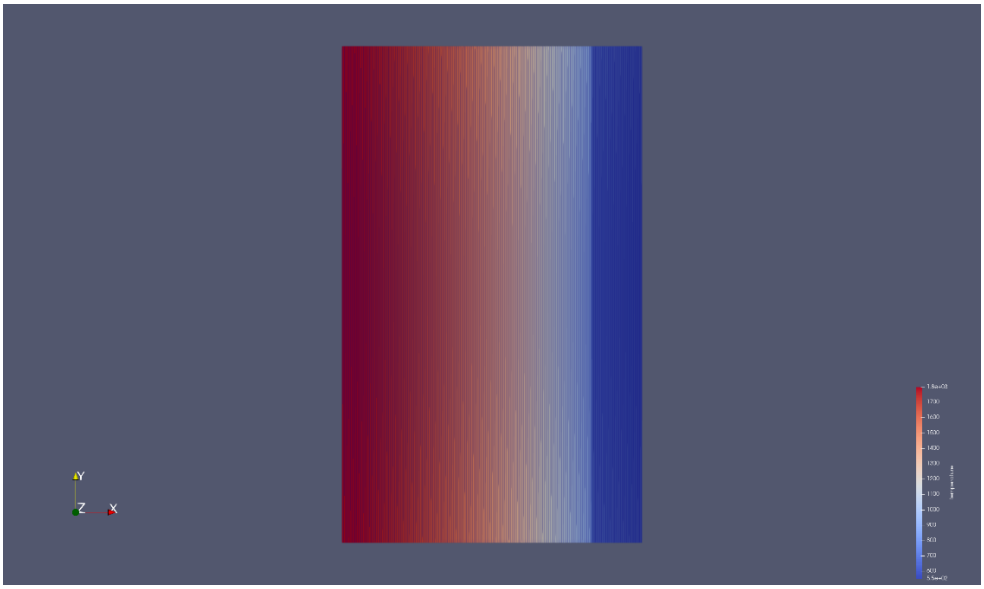

Fig.2. 2D image of steady state with constant k.

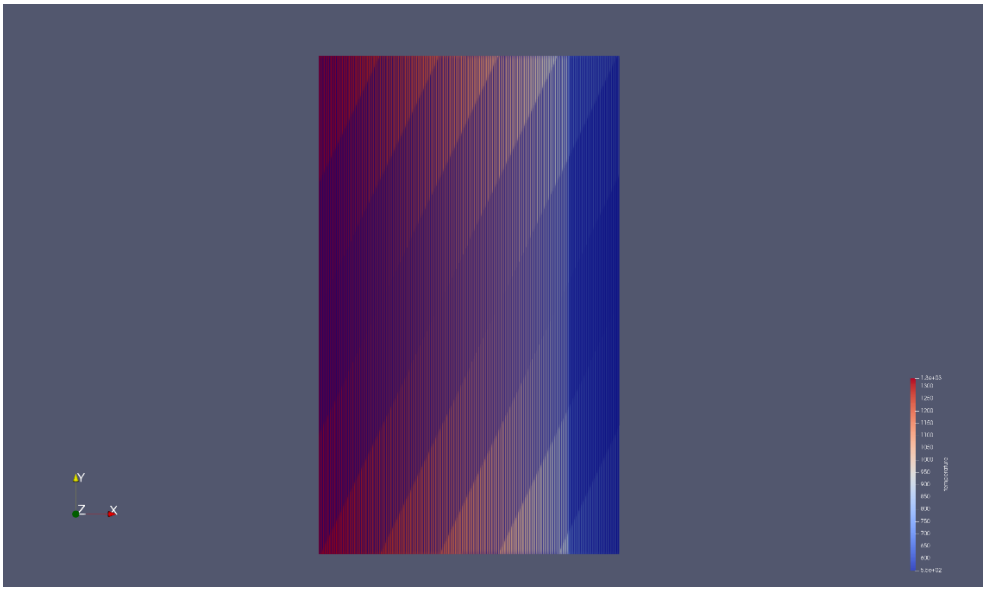

Fig.3. 2D image of steady state with temperature-dependent thermal conductivity.

Comparison with Analytical Solution:

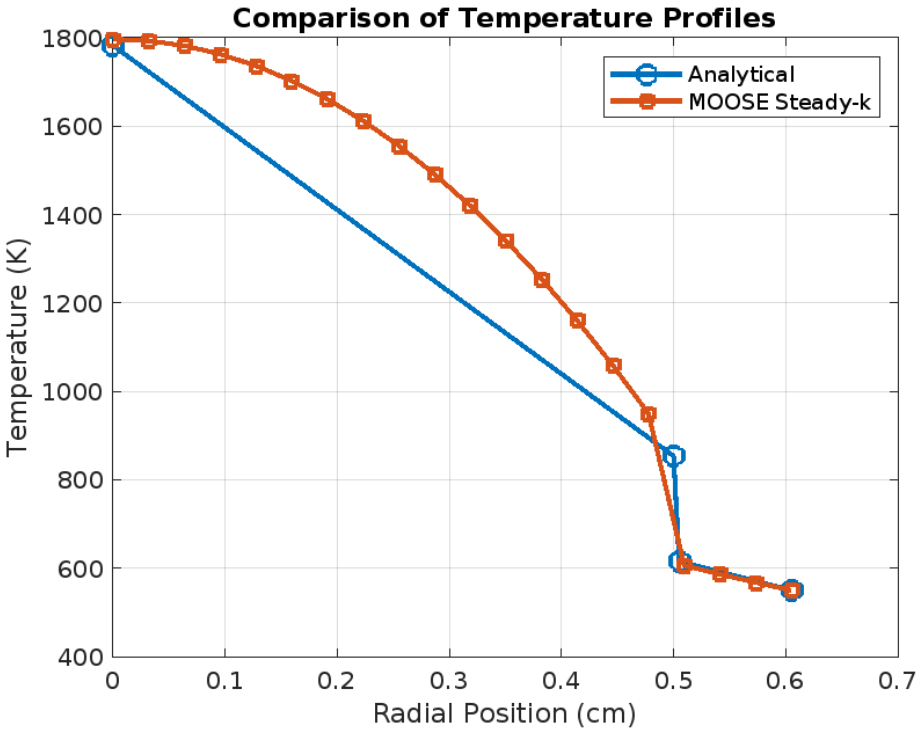

Fig.4. Analytical solution vs steady state with constant k.

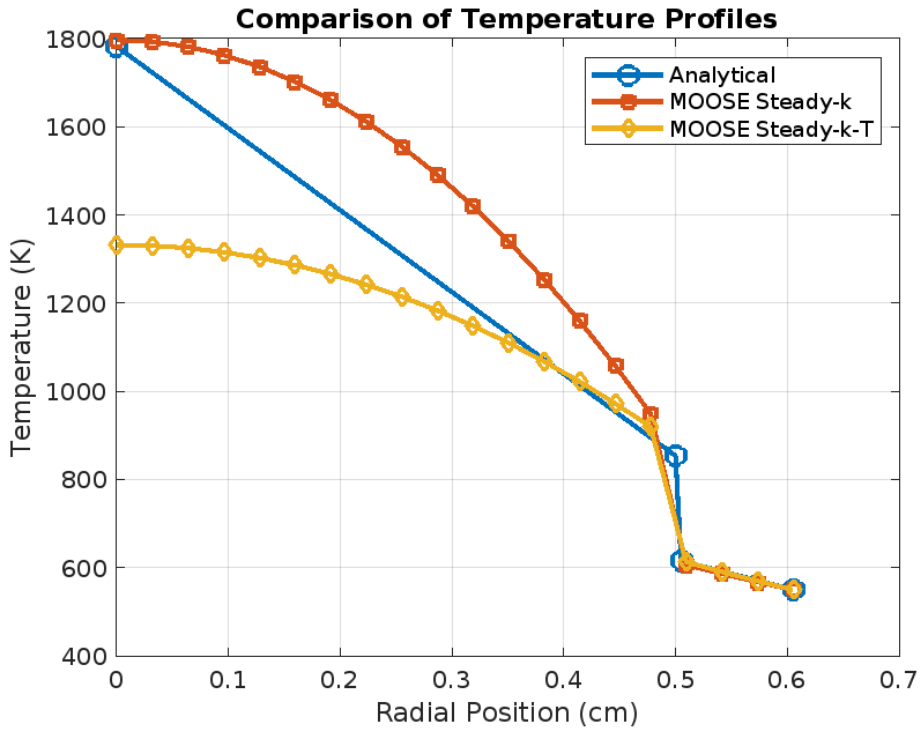

Fig.5. Analytical solution vs steady state with constant k vs steady state with temperature-dependent k

Key Observations

- The maximum temperature occurs at the fuel centerline.
- A significant temperature drop is observed across the gap region.
- The outer cladding temperature is maintained at 550 K, as specified by the boundary condition.

For the constant thermal conductivity case, the fuel centerline temperature predicted by MOOSE was **1796.79 K**, while the analytical solution yielded **1782.11 K**, showing a minor discrepancy of **14.68 K (0.8% difference)**. This variation arises due to numerical discretization errors and differences in boundary condition handling between the numerical and analytical methods. The comparison between the numerical and analytical results is illustrated in Fig.4.

However, when thermal conductivity was modeled as a function of temperature, the fuel centerline temperature significantly dropped to **1332.10 K**. This decrease is attributed to the increase in thermal conductivity from a constant **0.03 W/cm-K** to a temperature-dependent value reaching **0.0616 W/cm-K.** The higher conductivity enhances heat transfer within the fuel, effectively reducing the temperature gradient and leading to a lower centerline temperature. The impact of this variation is shown in Fig.5. , where the centerline temperature profiles for both steady-state cases are compared.

4.2. Transient with constant thermal conductivity and temperature-dependent thermal conductivity.

Visualization:

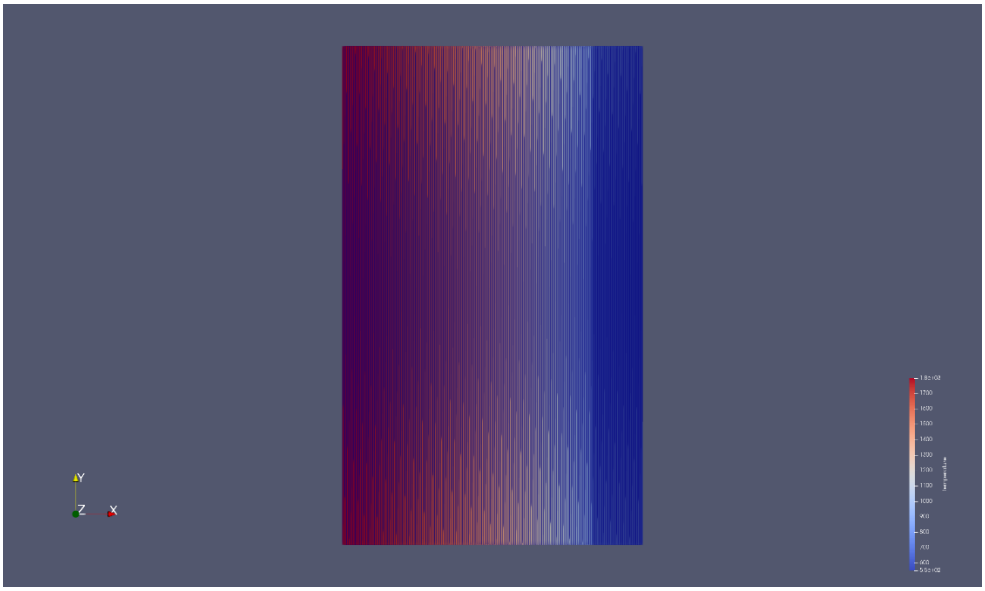

Fig.6. 2D image of transient with constant k.

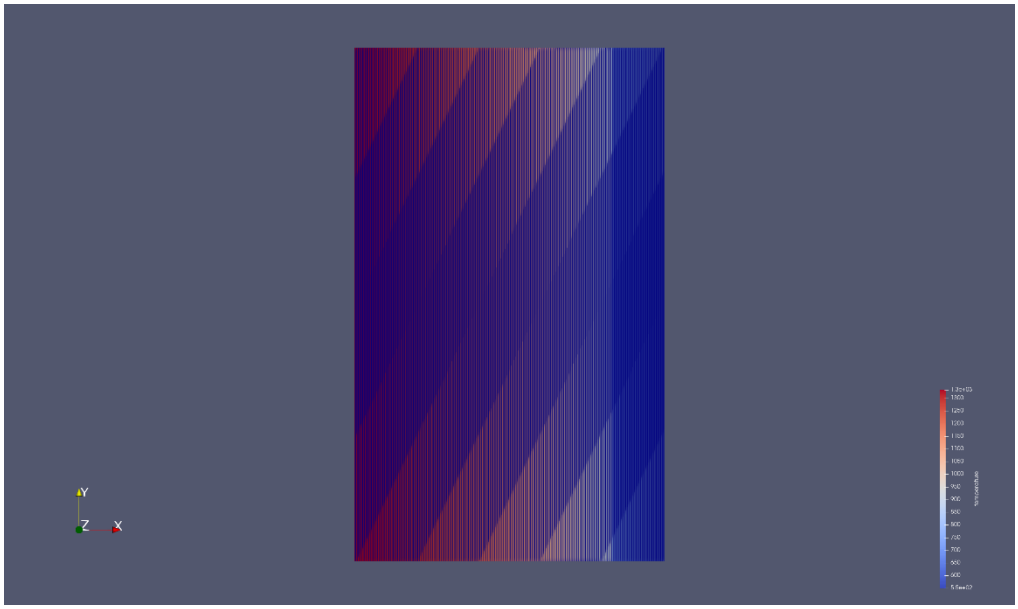

Fig.7. 2D image of transient with temperature-dependent thermal conductivity.

Temperature Evolution Over Time:

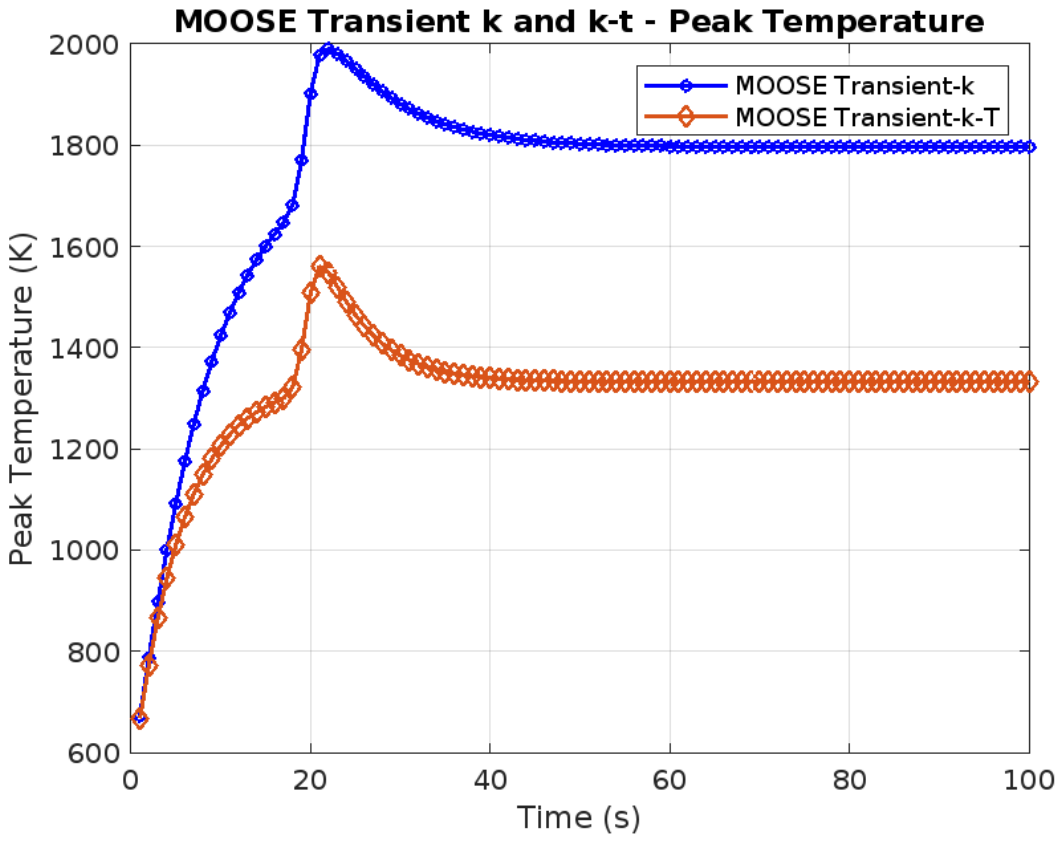

Fig.8. Transient with constant k vs transient with temperature-dependent k.

Peak Temperature values:

- **1989K** at 22nd time-step for transient with constant thermal conductivity.
- **1490K** at 24th time-step for transient with temperature dependent thermal conductivity.

Key Observation:

At the 100th time step, the fuel centerline temperature for the transient case with constant thermal conductivity was **1796.13K**, which closely matches the steady-state value of **1796.79K**. This agreement indicates that by this step, the system has nearly reached steady-state conditions, as expected in a well-converging transient simulation.

However, for the transient case with temperature-dependent thermal conductivity, the centerline temperature at the 100th time step was **1332.10K**, consistent with the steady-state result for the same thermal conductivity model. This significant drop, compared to the constant thermal conductivity case, is due to the increased thermal conductivity (from **0.03W/cm-K** to **0.0616 W/cm-K**) as temperature rises. The higher conductivity enhances heat dissipation, resulting in a lower temperature gradient and a reduced peak temperature.

The discrepancy between the two cases highlights the critical influence of temperature-dependent material properties on transient heat conduction, where an underestimation of thermal conductivity can lead to an overestimation of peak fuel temperatures and vice-versa.

Figures Fig.7. and Fig.8. illustrate the transient temperature evolution and comparison between constant and temperature-dependent thermal conductivity cases.

5. Conclusion

The steady-state and transient analyses show close agreement between the numerical and analytical data, with a minor discrepancy of 14.68 K (0.8%) in the steady-state case using constant thermal conductivity. This variation arises from numerical discretization. The reduction in fuel centerline temperature from 1796.79 K (constant conductivity) to 1332.10 K (temperature-dependent conductivity) emphasizes the importance of accurately modeling thermal conductivity to avoid overestimating peak temperatures.

In the transient analysis, the results closely align with the steady-state values by the 100th time-step, confirming thermal equilibrium. The discrepancy between the cases highlights the influence of temperature-dependent material properties on heat conduction and safety margins.

As a first-time MOOSE user, challenges included meshing, boundary conditions, and input configurations. Despite these hurdles, the results demonstrate MOOSE's effectiveness,

6. References

[1] Nuclear fuel performance model 1 lecture 3 (slide 15, 26 and 31)

[2] J. K. Fink. Thermophysical properties of uranium dioxide. *Journal of Nuclear Materials*, 279(1):1–18, 2000. https://doi.org/10.1016/S0022-3115(99)00273-1

[3] Thermal conductivity empirical models in BISON to compute UO2 thermal conductivity and its dependence on temperature, porosity, burnup for UO2 fuel. (MOOSE FRAMEWORK)

[4] NASAGRC. Space Nuclear Propulsion Material Property Handbook Revision 000. Technical Report, National Aeronautics and Space Administration Glenn Research Center, Cleveland, Ohio, 2020.

[5] MOOSE (Homepage)